RSC Advances

This is an *Accepted Manuscript*, which has been through the Royal Society of Chemistry peer review process and has been accepted for publication.

Accepted Manuscripts are published online shortly after acceptance, before technical editing, formatting and proof reading. Using this free service, authors can make their results available to the community, in citable form, before we publish the edited article. This *Accepted Manuscript* will be replaced by the edited, formatted and paginated article as soon as this is available.

You can find more information about *Accepted Manuscripts* in the Information for Authors.

Please note that technical editing may introduce minor changes to the text and/or graphics, which may alter content. The journal's standard Terms & Conditions and the Ethical guidelines still apply. In no event shall the Royal Society of Chemistry be held responsible for any errors or omissions in this *Accepted Manuscript* or any consequences arising from the use of any information it contains.

ROYAL SOCIETY OF CHEMISTRY

www.rsc.org/advances

Journal Name

RSCPublishing

ARTICLE

Graphene and Co-polymer Composite Based Molecularly Imprinted Sensor for Ultratrace Determination of Melatonin in Human Biological Fluids

Cite this: DOI: 10.1039/xoxxoooooox

Received ooth January 2012,
Accepted ooth January 2012

DOI: 10.1039/xoxxoooooox

www.rsc.org/

Pankaj Gupta[a], Rajendra N. Goyal[a]*

A novel molecularly imprinted polymer (MIP) sensor based on the composite of graphene (GR) and co-polymer of 4-amino-3-hydroxy-1-naphthalenesulfonic acid (AHNSA) and melamine (MM) has been fabricated for detecting the melatonin. The MIP film was fabricated by the deposition of graphene layer on a glassy carbon electrode (GCE) surface followed by electropolymerizing AHNSA and MM in the presence of melatonin. The morphology of the sensor was characterized by using Field Emission-Scanning Electron Microscopy (FE-SEM) and Electrochemical Impedance Spectroscopy (EIS). The electrochemical performance of the imprinted sensor was investigated by using cyclic voltammetry and square wave voltammetry. The electropolymerization conditions, method of template removal, effect of template to monomer ratio and incubation time were optimized. Electrochemical results showed that the oxidation peak current increased linearly with the concentration of melatonin in the range 0.05 to 100 μM L^{-1}. The detection limit of the imprinted electrochemical sensor towards the melatonin determination is calculated to be 60×10^{-10} mol L^{-1}. The suitability of GR/MIP based sensor has been demonstrated in detecting the melatonin in biological samples.

Introduction

Melatonin (N-acetyl-5-methoxytryptamine), a naturally produced indoleamine hormone, is biosynthesized from tryptophan via serotonin in reactions catalyzed by serotonin N-acetyltransferase and acetylserotonin O-methyltransferase. It is secreted by the vertebrate pineal gland situated in the brain and stimulates in darkness (200 pg/ml) and suppressed by daylight (10 pg/ml), thereby regulating the circadian rhythm [1-3]. Melatonin is used as a chronobiotic that is capable of normalizing the disturbed circadian rhythms, including sleep-wake rhythms and imbalances imposed by jet lag or shift work. Melatonin is also implicated in the regulation of mood, learning and memory, immune activity, dreaming, fertility and reproduction [1, 4-5]. In mammals, melatonin activates G protein-coupled receptors, the melatonin receptor 1 (MT_1) and melatonin receptor 2 (MT_2), present in many regions of the central nervous system and exert cellular and physiological actions including neuronal firing, arterial vasoconstriction, cell proliferation, immune responses, reproductive and metabolic functions [6]. Melatonin also behaves as an effective antioxidant and anti-inflammatory hormone that enhances the activity of antioxidant enzymes and diminishes oxidative injury [7, 8]. It has been found to act as a neuroprotective agent in Alzheimer and Parkinson's disease models and an immunomodulator in cancer therapy [9, 10]. Exogenous melatonin has an estimated oral bioavailability of 40–70% for doses of 2.5–μ100mg and the time to peak plasma concentration of exogenous melatonin has been estimated as 60-150 min, after its administration and the elimination half-life is 20-50 min [11, 12].

Due to its significant role in human physiology, neuroscience and clinical diagnosis, several analytical techniques have been employed for the melatonin determination in biological and pharmaceutical samples. These techniques include HPLC with electrochemical and fluorometric detection, gas chromatography-mass spectrometry, micellar electrokinetic chromatography, spectrofluorimetry, chemiluminescence, radioimmunoassay and colorimetry (13-20). However, most of these techniques require expensive devices with sophisticated processes and maintenance along with complicated, tedious and time consuming derivatization and extraction steps. In addition these techniques require organic solvents for separation and, thus cause environment pollution. Electrochemical techniques on the other hand are reported as ecofriendly and considered as highly sensitive, selective and convenient tool with fast response and low cost as compared to the other routine analytical techniques [21]. Various modified electrodes, such as boron doped diamond electrode [11], carbon ionic liquid electrode modified with carbon nanotubes (CNTs) and cobalt hydroxide nanoparticles [4], drug membrane sensors, carbon paste electrode and glassy carbon electrodes modified with CNT's [3, 22-26] have been used for the melatonin determination. However, the presence of higher concentration of some metabolites such as ascorbic acid and uric acid strongly interfere in the selective determination of melatonin in biological samples. Thus, the aim of this study was to prepare a sensor for the selective and sensitive determination of melatonin in human biological fluids.

RSC Advances Accepted Manuscript

As a typical approach for high affinity and specific recognition, molecularly imprinted polymers (MIPs) have gained a considerable attention in the recent years and have been found most promising in the field of artificial molecular recognition systems [27]. In place of biological recognition system, like antibody-antigen and enzymes, the MIPs have several potential advantages such as stability, predictable specificity, durability, affordability, easy preparation and lower-cost. These qualities make them an important and attractive tool in the form of artificial and robust recognition materials [28, 29]. In order to generate imprints with certain selectivity, a prepolymer is simply polymerized with a desired target molecule, which acts as a molecular template. During polymerization, functional groups in the prepolymer orient toward their counteracting partners in the template and this orientation remain as such, even when the template is removed. The cavities of the prepared polymer film, after extraction of the template, possessed both the correct shape and the correct orientation of the functional groups and allowed them to distinguish template molecules through their stereoconfiguration. As a new class of materials possessing high selectivity and affinity for the target molecule, MIPs have been widely applied in the sensor development [30, 31].

Graphene (GR), a two-dimensional planar sheet of sp^2 bonded carbon atoms, densely packed in a honeycomb crystal lattice structure has high thermal conductivity, electrical conductivity, large accessible surface area, very efficient electrocatalytic behavior and good biocompatibility. Because of its outstanding properties, GR attracted considerable focus for its applications in energy storage, photovoltaic devices, nanocomposites, nanoelectronics, bioelectronics and biosensing [32-35]. MIP film fabricated on the surface of GR sheet has been proved as an excellent polymer nanocomposites surface for target species with higher affinity and sensitivity. Due to these features application of graphene as supporting material in the preparation of MIPs has been investigated [36-38]. As compared to other methods, like drop coating, composite membrane technique, an electropolymerization method has been found to have several advantages, such as high fabrication rates, low material consumption and controllable film thickness and morphology [39].

In this article, we have described a rapid, selective, sensitive and cost effective method based on MIP for the determination of melatonin. The GR as a supporting material, melatonin as template molecule, 4-amino-3-hydroxy-1-naphthalenesulfonic acid (AHNSA) and melamine (MM) as the monomers have been used to construct the MIP film on the surface of glassy carbon electrode. AHNSA and MM have been extensively used in MIP studies, however, in the present studies individual use of these monomers did not exhibit a significant increase in the peak current of melatonin. Hence, an attempt to use both of these monomers to form a copolymer was made and a remarkable increase in the peak current was noticed. The proposed sensor (GCE/GR/MIP) exhibited large number of recognition sites for the melatonin, along with good stability and reproducibility. The results showed that the proposed sensor had good analytical performances such as sensitivity, selectivity and rapid response toward melatonin determination.

Experimental

2.1 Reagents and materials

Melatonin, AHNSA, melamine, graphite powder (< 20 μm), ascorbic acid, uric acid sulphuric acid and nitric acid were purchased from Sigma-Aldrich Chemical Co, USA. All the chemicals used to prepare phosphate buffers in the pH range 2.4–10.0 were obtained from E. Merck (India) Ltd. Mumbai. Phosphate buffers of ionic strength (1.0 M) were prepared according to the reported method [40]. The urine and blood samples of patient undergoing treatment with melatonin were obtained from the Institute hospital of IIT Roorkee, after the permission of the human ethical clearance committee of IIT Roorkee. The samples were obtained after 2 h of oral administration of melatonin and were stored in the refrigerator immediately after collection. The plasma was separated by centrifugation and used for the determination of melatonin. Urine and plasma samples were suitably diluted to minimize matrix complexity. The solution to be analyzed was transferred into the voltammetric cell without any further pretreatment. The standard addition method was used for the determination of melatonin in real samples. Melatonin containing tablets manufactured by different companies were purchased from the local market of Roorkee. All other chemicals and solvents used in the experiment were of analytical grade and double distilled water was used throughout the experiments.

Apparatus

All the voltammetric experiments were performed with a computerized Bio Analytical System (BAS, West Lafayette, USA) Epsilon voltammetric analyzer. A conventional single compartment three electrode glass cell, equipped with GCE/GR/MIP sensor as the working electrode, Ag/AgCl (3 M NaCl) reference electrode (BAS Model MF-2052 RB-5B) and a platinum wire as the counter electrode was used. The pH measurement was performed using Thermo Fisher Scientific, Singapore Digital pH meter (Eutech Instruments, model pH 700). The Field Emission-scanning Electron Microscope (FE-SEM) images were taken by the Zeiss ultra plus 55. Electrochemical Impedance Spectroscopy (EIS) was performed on galvanostat (model; Versastat 3, PAR). Powder X-ray diffraction (XRD) measurements were performed using Bruker D8-advance X-ray powder diffractometer. Raman spectroscopic measurements were performed on Renishaw invia Raman microscope. UV-VIS. spectroscopy was performed using Shimadzu spectrophotometer (UV-VIS) model UV-2450.

Preparation of graphene

The graphene was synthesized using the improved Hummers method [41]. Typically for the synthesis of graphene oxide (GO), 9 g of $KMnO_4$ and 1.5 g of graphite powder were mixed in the solution of H_3PO_4 and H_2SO_4 (20:180) mixture. The solution was heated to 50 ºC and kept stirring for 12 h, after which a dark brown colored material was obtained. Next, addition of 100 mL of distilled water followed by the slow addition of 1.5 mL of H_2O_2 (30%), turned the color of the solution to yellow. After centrifugation and then sedimentation, the material obtained was washed with 200 mL of water followed by washing with 100 mL of HCl (30%). Further washing was done with 200 mL of ethanol and final sediment so obtained was GO. For the synthesis of graphene, reduction of GO was carried out by sonicating the mixture of 20 mL water, 50 mg GO and 0.5 mL of hydrazine for 1 h followed by stirring for 24 h at 50 ºC. After filtration black powder of graphene was obtained, which was dried in vacuum. GO and

RSC Advances Accepted Manuscript

 This journal is © The Royal Society of Chemistry 2012

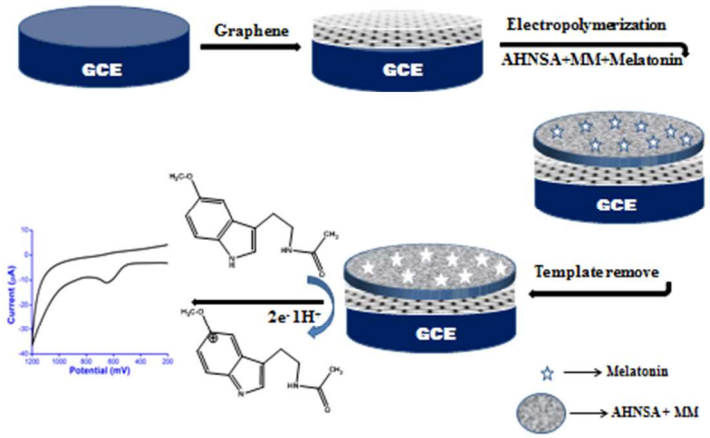

Scheme-1: Graphene and Co-polymer composite induced surface for specific determination of melatonin.

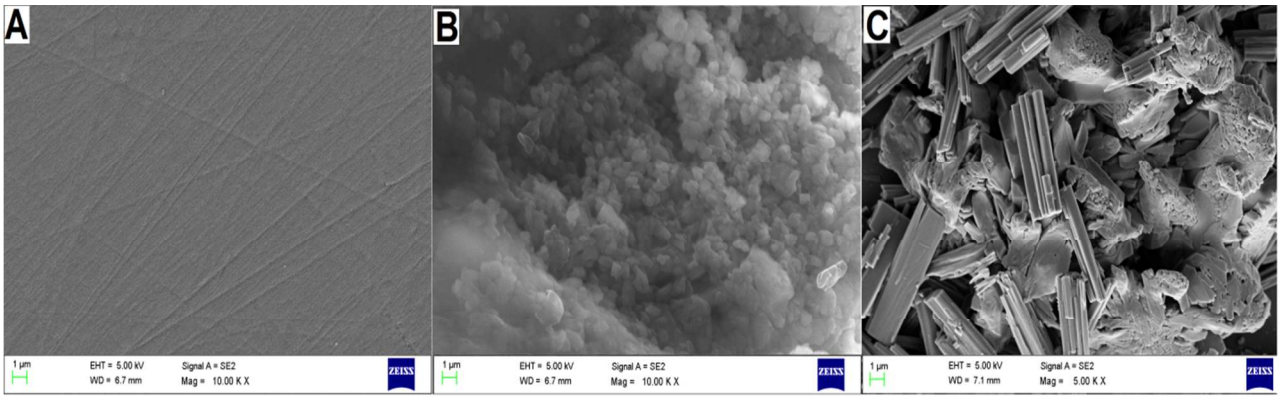

Fig.1 FE-SEM images observed for (A) Bare GCE (b) GR/ GCE (C) AHNSA-MM/GCE.

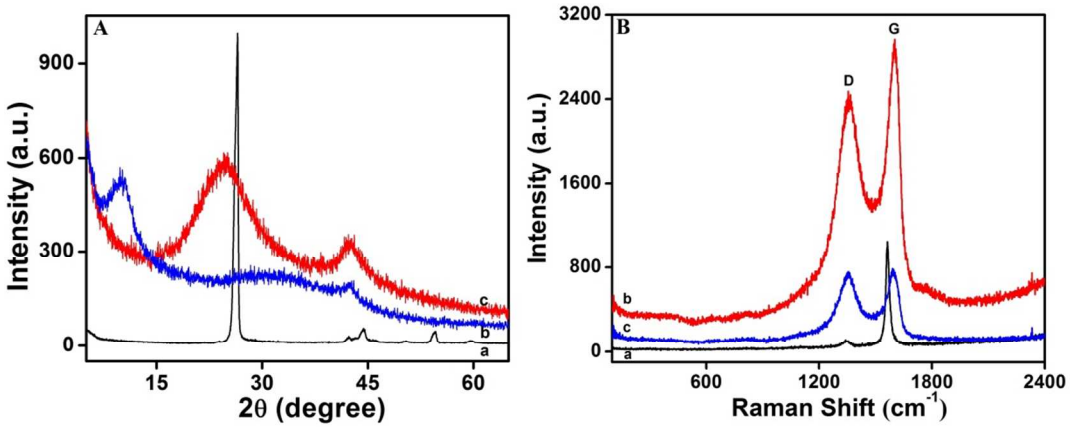

Fig.2 (A) XRD pattern and (B) Raman spectrum observed for (a) Graphite, (b) GO and (c) GR

graphene as obtained were characterized using XRD and Raman spectroscopic measurements.

Preparation of graphene modified imprinted and non-imprinted sensor

For the fabrication of GR/MIP film on GCE, the surface of the glassy carbon was first polished with a paste of alumina powder (grade I) and ZnO on micro cloth pad to a mirror like finish surface and then it was rinsed with double distilled water. The construction of the GCE/GR/MIP mainly included three steps as follows (Scheme 1). Firstly, 10 µl of the ultrasonically dispersed graphene in a mixture of double distilled water and DMF (1: 9) at a concentration of 0.7 mg mL^{-1} was dropped on the surface of freshly cleaned GCE and dried at room temperature overnight [42]. Secondly, the film of imprinted copolymer was prepared by the electropolymerization of

RSC Advances Accepted Manuscript

AHNSA and melamine on the surface of graphene modified GCE. For this purpose, 0.01 M solution of AHNSA and MM were prepared in 0.1 M HNO_3 and 0.1 M H_2SO_4, respectively. A 0.005 M solution of melatonin was used for MIP synthesis. The polymerization was carried out in a solution containing 2 ml melatonin, 1 ml AHNSA and 1 ml of melamine monomer by using cyclic voltammetry in the potential range -0.8 V and +2.0 V at a scan rate of 100 mV s^{-1} for optimized 20 scans [43, 44]. The film obtained was rinsed with double distilled water. Finally, modified electrode was cycled between -1.0 and +1.0 V at a scan rate of 100 mV s^{-1} for 25 cycles in 0.5 M H_2SO_4 to release the imprinted melatonin molecules from the composite. A non-imprinted polymer sensor (GCE/GR/NIP) was constructed under identical conditions except that the template molecule was absent in the electropolymerization step. The surface morphology of the bare and modified sensors at different stages was studied using FE-SEM and a comparison of the microscopic images observed is shown in Fig. 1. The deposition of GR as flakes and copolymerization of AHNSA and MM at GCE surface can be clearly seen as shown in Fig. 1. The rod shape structures in Fig 1 belong to AHNSA, while others are melamine, which was confirmed by separate SEM images of the individual polymers. The electro-polymerization was carried out by cyclic voltammetry, hence partial co-polymerization of monomers took place. Thus, the SEM image shown in Fig 1C is not homogeneous

Voltammetric procedure

Stock solution of melatonin (1 mM) was prepared by firstly dissolving the required amount in a minimum amount (0.5 mL) of ethanol and then water was added upto the mark and the colourless solution obtained was stored in a refrigerator. For recording the voltammograms, required amount of the solution was added to the cell containing 2 ml of buffer and total volume was made to 4 ml using double distilled water. The imprinted sensor was then dipped in this solution for 4 min after which it was washed with double distilled water and then voltammograms were recorded under optimized parameters. The binding of melatonin with GCE/GR/MIP was strong, hence, it was removed by time base technique in which a potential of -800 mV was applied for 150s. The optimized square wave voltammetric parameters used were initial (E): 0 mV, final (E): 1000 mV, square wave amplitude (E_{sw}): 25 mV, potential step (E): 4 mV and square wave frequency (f): 15Hz. All potential reported are with reference to the Ag/AgCl electrode at an ambient temperature of 25 ± 2 °C.

Result and discussion

Characterization of graphene and GR/MIP film

The XRD pattern observed for graphite oxide and graphene is presented in Fig. 2. GO exhibits a peak centered at 2h = 10.4°, corresponding to the (002) plane (Fig. 2A curve b). After chemical reduction with hydrazine, graphite oxide was reduced to graphene nanosheets with a character peak at 2h = 24.7° with increased inter-planar spacing, which is larger than that of ordinary graphite as shown by curve C in Fig. 2A [42].

The defect in the crystal structures of carbon during the synthesis of graphene from graphite was studied by Raman spectra. The changes in the relative intensity of two main peaks: D and G spectra were observed as shown in Figure 2B. The D band originating from the edges can be attributed to the defects in graphene nanosheets and G band, which is in-plane vibration of sp^2 carbon atoms, can be used to explain the graphene layer thickness. A comparison of the spectra of graphite (curve a), GO (curve b) and GR (curve c) shows that D-band at ~1354 cm^{-1} for GO and graphene shows larger intensity than graphite and an increment in D peak intensity confirms the formation of more sp^2 domains. On the other hand, the G peak at around 1603 cm^{-1} for GO and at 1597 cm^{-1} for graphene is assigned to the first order scattering of the E2g phonon of sp^2 C atoms, revealing decrease in number of layers in the flake [42, 45].

EIS is an effective method, which provides detailed information about the electron transfer at the interface of electrode and solution. The surface morphology of the imprinted and non-imprinted sensors in terms of the impedance changes was carried out in the 1:1 solution of 5 mM $K_3Fe(CN)_6$ and 0.1 M KCl over the frequency range of 100 kHz to 10 mHz at a potential of 0.05 V. Randle's equivalent circuit was used to obtain EIS spectra; where (Rs) was the ohmic resistance of the electrolyte solution; (C_{dl}) was the double layer capacitance and (R_{ct}) was the electron transfer resistance. The semicircle portion at higher frequency represents R_{ct} and the linear part is due to the diffusion process and represents Warburg (Z_W) resistance. The results were found to fit best to a simple Randles equivalence circuit.

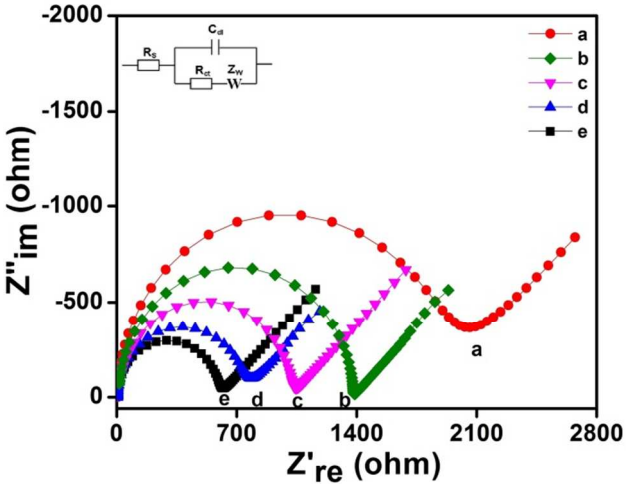

Fig.3 Nyquist-diagram for the electrochemical impedance measurement observed for GCE (a), GCE/NIPs (b), GCE/MIPs (c), GCE/GR-MIPs before extracting template (d), and after extracting template (e). The inset represents Randle's equivalent circuit.

Fig. 3 shows the Nyquist plot of EIS observed for bare GCE (a), GCE/NIPs (b), GCE/MIPs (c), GCE/GR-MIPs before extracting template (d), and after extracting template (e). As presented in Fig. 3, R_{ct} of bare GCE was found to be 1855 Ω, which was higher in comparison to the modified sensors (curve a). After modification of the GCE surface with MIP and NIP film, the R_{ct} values decreased indicating thereby that NIP film has higher resistance value in comparison to the MIP film (curve b and c). This behavior can be explained on the basis that the NIP film has no available recognition site and hence, resist the electron-transfer kinetics of the redox probe at the electrode-solution interface. After incorporation of GR, resistance value significantly decreased implying that the graphene film formed high electron conduction pathways (curve d and e). After removal of the template from the GCE

RSC Advances Accepted Manuscript

This journal is © The Royal Society of Chemistry 2012

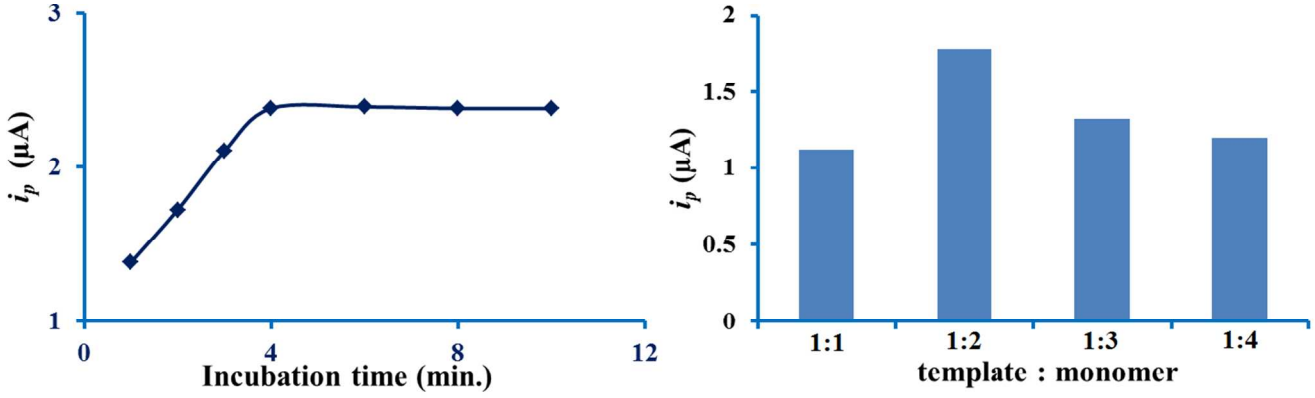

Fig.4 (A) Effect of incubation time on the peak current response of 10 μM melatonin observed using the imprinted sensor at pH 7.2. (B) Effect of template to monomer concentration ratio on the response of sensor to melatonin.

/GR-MIP sensor, the R_{ct} values substantially decreased to 590 Ω from 726 Ω, due to the exposure of the formed recognition sites or the binding cavities.

Optimization of experimental conditions

The incubation step is usually an efficient way to enhance the sensitivity of a MIPs sensor as it influences the interaction between imprinted film and analyte molecules. The effect of incubation time on binding capacity of melatonin was evaluated by immersing the proposed sensor into 10 μM concentration of melatonin from 1 min to 10 min and the current response was measured in phosphate buffer solution of pH 7.2. It was observed that the peak current increased with increase in 4 min after which, the peak current remained practically constant (Fig. 4A). This behavior can be explained on the basis that all molecular recognition sites of the sensor get saturated by melatonin molecules and hence the current becomes constant. Thus, incubation time of 4 min was optimized for the subsequent studies. The sensitivity of the imprinted sensor is prescribed by the amount of effective imprinted sites on the sensor surface and to generate the imprinted sites on the sensor surface, the concentration ratio of template to monomer is found to play a key role. Therefore, to achieve the maximum sensitivity, the optimization was done by varying the concentration of the monomers up to 4 times in comparison to the template. For this experiment, the total volume of solution was taken 4 ml (2 ml melatonin, 1 ml AHNSA and 1 ml of melamine monomer). It was observed that the largest peak current response of imprinted film was obtained when it was synthesized by the solution having two times greater concentration of monomers in comparison to template (1:2). One of the reasons for highest absorbance at around 279 nm in 1:2 composition is maximum binding of template to monomers. During the equal concentration of template and monomers (1:1), the current response was very small because of the limited amount of monomer available for combining to template molecules. On the other hand at the higher concentration of monomers (upto 3 and 4 times), the peak current again decreased as the imprinted membranes were too thick and binding sites were difficult to access by template molecules. The dependence of melatonin current response on the template-monomer concentration is presented in Fig. 4B. These results were further supported by UV-VIS spectroscopy. The MIP film was prepared on GR modified GCE with 1:1 to 1:4 concentration ratio of template to monomers. To release the imprinted molecules from the film, the sensors were scanned in between the potential range of -1.0 and +1.0 V at a scan rate of 100 mV s^{-1} for 25 cycles in 0.5 M H_2SO_4. The H_2SO_4 solutions were used for recording UV-Vis spectra. A typical UV absorption spectrum of melatonin solution shows a peak at 279 nm as shown in the inset of Fig. 5. It was observed that the imprinted film with 1:2 templates to monomer concentration ratio had highest absorbance at 279 nM and thus had the highest number of binding site with template molecules (curve b). A comparison of UV spectra for H_2SO_4 solutions obtained from different ratio of template to monomer is presented in Fig. 5. The inset of Fig. 5 shows the spectrum for standard 100 μM melatonin and the calibration curve, which is obtained from the UV spectra of melatonin in the concentration range of 0.5 μM to 100 μM. The linear regression equation for the calibration curve can be represented as:

$$\text{Absorbance} = 0.0094\ C\ (\mu M) + 0.0372$$

having correlation coefficient of 0.997. By using this equation, the concentration of melatonin, which was released from the imprinted film cavity, was found to be 25 μM (curve b).

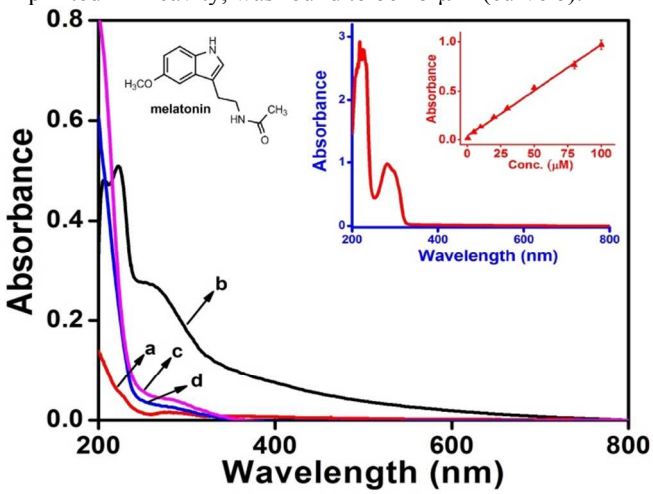

Fig.5 Electronic absorption spectra of template melatonin in the solution of H_2SO_4 released from MIPS prepared with template to monomer ratio of template to monomer (a) 1:1 (b) 1:2 (c) 1:3

RSC Advances Accepted Manuscript

(d) 1:4. The inset represents the spectrum for standard 100 μM melatonin and a calibration plot of 0.5 μM to 100 μM of melatonin.

Electrochemical characterization

Cyclic voltammetry

The cyclic voltammograms of melatonin were recorded at GCE/MIP, GCE/GR/NIP and GCE/GR/MIP sensors in the phosphate buffer of pH 7.2. A comparison of cyclic voltammograms observed is shown in Fig. 6. At all the sensors melatonin is irreversibly oxidized giving a single oxidation peak with peak potential of ~733 mV, ~672 mV, ~665 mV and ~648 mV at bare GCE, GCE/MIP, GCE/GR/NIP and GCE/GR/MIP sensors respectively. A poor broad response for the oxidation of melatonin was observed at bare GCE in comparison to the modified sensors. At GCE/MIP, a well-defined oxidation peak was observed (curve c), however, after modification with graphene, the peak current of melatonin significantly increased (curve d). The electrochemical response of the GCE/GR/NIP was also examined and it was found that the anodic peak of melatonin shifted to negative potentials but the peak current did not show any increase as compared to GCE/MIP due to the absence of binding sites. Under the similar conditions, it was noticed that the peak current of melatonin at the GCE/GR/MIP was higher with negative shift of peak potential than that obtained at the GCE/MIP and GCE/GR/NIP. This behaviour indicated that the template melatonin imprinted procedure was successful and the remarkable enhancement of the peak current and negative shift of anodic peak potential was clear evidence of electrocatalytic effect of GR to the oxidation of melatonin. To ascertain the nature of the electrode reaction, scan rate studies were performed in the range of 10–200 mV s^{-1}. The peak current of melatonin was found to increase linearly with increase in the sweep rate and the dependence of the anodic peak current on scan rate can be expressed by the relation:

i_p (μA) = 0.040[v] + 0.669

having a correlation coefficient of 0.998, where v is the scan rate in mV/s and i_p is the peak current in μA. The linear relation of i_p versus scan rate plot (inset of Fig. 6) indicated that oxidation of melatonin is adsorption controlled at GCE/GR/MIP which was further confirmed by the linearity of $i_p/v^{1/2}$ vs. log v and log i_p vs. log v plots. The dependence of log i_p on log v can be expressed by the relation:

log i_p = 0.747 log v - 0.809

with a correlation coefficient 0.997. The slope value (>0.5) of log i_p vs. log v plot further confirmed that the oxidation of melatonin involved adsorption complications [39].

Square wave voltammetry

As square wave voltammetry (SWV) is a more sensitive technique than cyclic voltammetry, further studies are carried out using SWV. Square wave voltammograms of 100 μM melatonin were recorded at bare GCE, GCE/MIP, GCE/GR/NIP and GCE/GR/MIP sensor surfaces in phosphate buffer solution of pH 7.2 using the optimized parameters of SWV. At bare GCE, a poor voltammetric response was

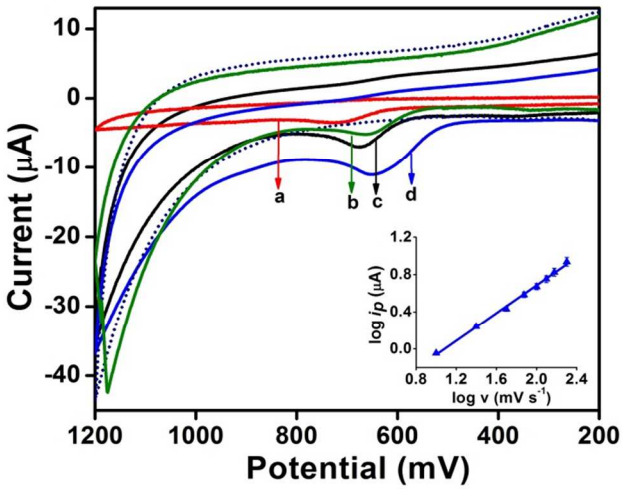

Fig.6 Typical cyclic voltammograms observed for 100 μM melatonin using (a) bare GCE, (b) GCE/GR/NIP, (c) GCE/MIP and (d) GCE/GR/MIP in phosphate buffer of pH 7.2 at a scan rate of 100 mVs^{-1}. Inset represents a graph between log i_p and log ν. The background is shown by the dotted line.

observed with a low peak current (i_p), whereas, at GCE/GR, GCE/MIP and GCE/GR/NIP a sharp peak due to oxidation of melatonin was observed at less potential in comparison to GCE. (Fig.7, curves b - d). At GCE/GR/MIP sensor, the E_p of

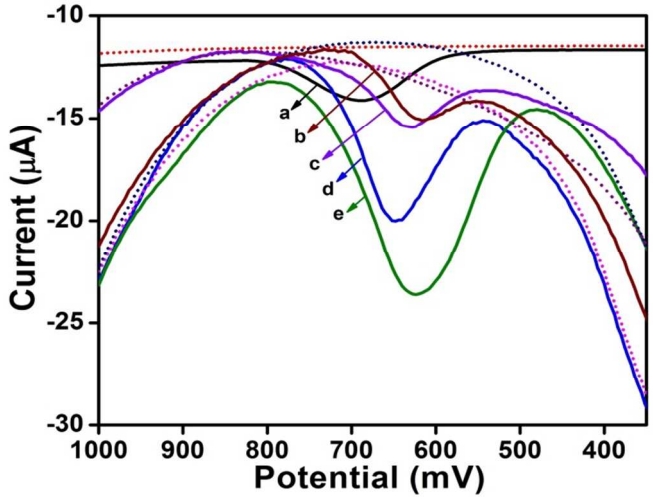

Fig.7 A comparison of SWVs observed for 100 μM melatonin at (a) bare GCE (b) GCE/GR, (c) GCE/GR/NIP, (d) GCE/MIP and (e) GCE/GR/MIP. The background is shown by the dotted line.

melatonin further shifted to more negative potentials with increase in peak current (curve e). This suggests that though GCE/GR catalyze the oxidation of melatonin the catalysis is lesser than observed in the case of GCE/GR/MIP. The excellent sensitivity of the GCE/GR/MIP toward melatonin can be attributed to the recognition sites situated in the MIPs film. These recognition sites complimented the molecular shape, size, and functionality of the template molecule, resulting in the specific binding ability of melatonin.

RSC Advances Accepted Manuscript

This journal is © The Royal Society of Chemistry 2012

Effect of pH

Table 1. A comparison of the working range and detection limit of melatonin at imprinted sensor with recently reported methods.

Sr. No.	Electrode Type	pH	Linear range	Detection Limit	Reference
1.	Carbon paste	1.7	3-550 µM	2.3 µM	[3]
2.	CIL/MWCNTs-CHNPs	7.5	0.01-50 µM	0.004 µM	[4]
3.	BDD	3.0	0.5-4 µM	0.11 µM	[11]
4.	AGCE	6.7	0.8-10 µM	0.05 µM	[22]
5.	BT-drug membrane sensors	5.0	1-0.10^4 µM	7 µM	[23]
6.	MWNTs-DHB/GCE	7.5	0.08-10µM	0.02 µM	[24]
7.	GCE	4.3	10-500 µM	1.48 µM	[25]
8	GCE/GR/MIP	7.2	0.05-100 µM	0.006 µM	Present work

The influence of pH on the anodic peak potential of melatonin was determined by using square wave voltammetry at imprinted sensor in the pH range 2.2–10.0. It was observed that the peak potential (Ep) of melatonin shifted to less positive potentials with increase in pH. The dependence of pH on the peak potential was linear and can be expressed by the relation:

E_p (pH 2.2-10) = [-37.52 pH + 889.23] mV vs. Ag/AgCl

having correlation coefficient of 0.998. The value of d*Ep*/dpH~ 37.52 mV/pH suggests that the number of electrons transferred in the oxidation of melatonin is double that of protons as reported in the literature [3, 4].
The dependence of the anodic peak current of melatonin on the square wave frequency was studied in the range 5–50 Hz using imprinted sensor. The peak current was found to increase linearly with square wave frequency and the linear relation between i_p and f can be expressed by the equation:

i_p (µA) = 0.1948[f] + 2.12

having a correlation coefficient of 0.990. This is in agreement with an adsorption controlled electrode reaction, which supports the inferences obtained from cyclic voltammetric studies.

Calibration curve for GCE/GR/MIP

To investigate the practical applications of the imprinted sensor for melatonin determination, the dependence of the oxidation peak current on the concentration of melatonin was examined in the phosphate buffer solution of pH 7.2. Fig. 8 shows the square wave voltammograms observed for various concentration of melatonin at the GCE/GR/MIP. The oxidation peak current (E_p~625 mV) increased linearly with increasing the melatonin concentration. The inset of Fig. 8 shows the corresponding calibration curve, demonstrating that in the range 0.05 µM to 100 µM, the anodic peak current has a good linear relationship with melatonin concentration. The linear regression equation can be represented as:

i_p (µA) = 0.1408 C (µM) + 0.8531

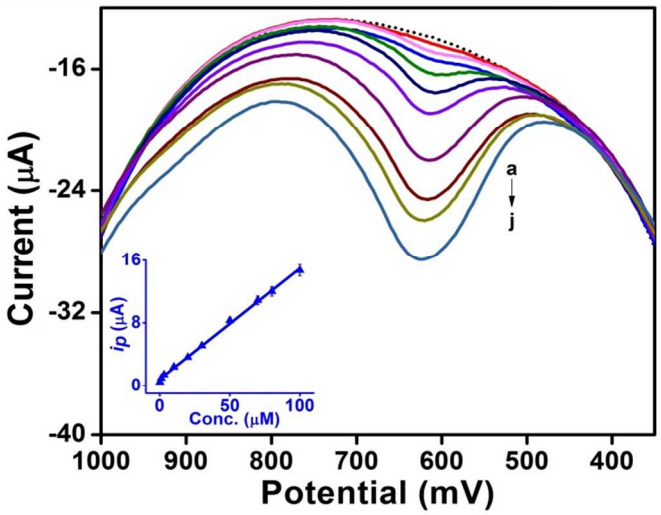

Fig.8 Square wave voltammograms recorded for increasing concentration of melatonin (a) 0.05; (b) 1; (c) 3; (d) 10; (e) 20; (f) 30; (g) 50; (h) 70; (i) 80; (j) 100 µM at GCE/GR/MIP in phosphate buffer of pH 7.2. Inset is the observed calibration plot between [C] and i_p. (Incubation time: 4 min.).

having a correlation coefficient of 0.998. The detection limit at imprinted sensor was evaluated by using the relation 3σ/b, where σ is the standard deviation of the blank solution and b is the slope of the calibration curve and was found to be 60×10^{-10} M. The detection limit of the presented sensor was also compared with reported in the literature in recent years and is summarized in Table 1. It can be seen that GCE/GR/MIP offered a wider linear range and an excellent lower detection limit than reported earlier.

Selectivity

Selectivity is an important indicator in order to test the practical application of the sensor. The interference substances are present in biological fluids and may interfere with the determination of melatonin through conventional methods. The selectivity of the imprinted sensor in this work was evaluated in the presence of main interfering molecules like ascorbic acid

RSC Advances Accepted Manuscript

(AA), uric acid (UA), xanthine (XA), tryptophan (TP) and guanine (GA) present in the biological fluids. Among various

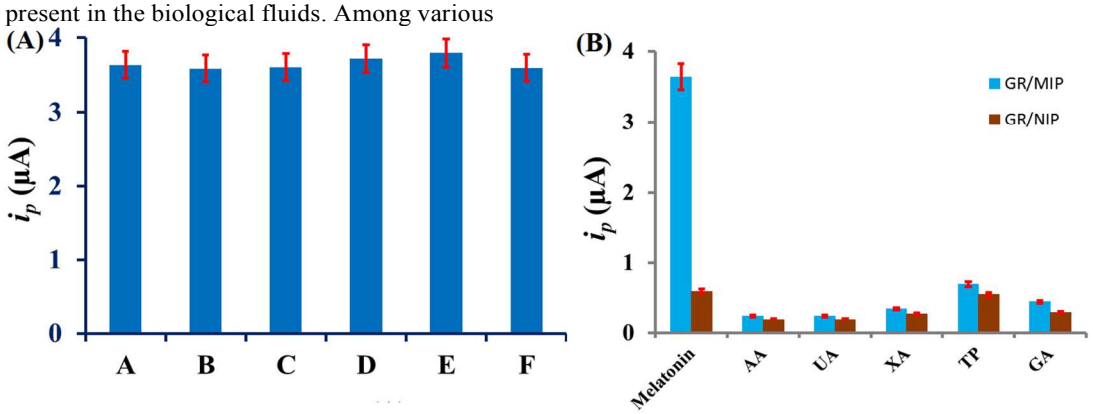

Fig.9 (A) Observed selectivity of imprinted sensor for 20 μM melatonin with (A) blank solution, (B) 1000 μM ascorbic acid, (C) 2000 μM uric acid, (D) 100 μM xanthine, (E) 100 μM tryptophan and (F) 100 μM guanine. (Incubation time: 4 min.). (B) Selective adsorption of melatonin by GCE/GR/MIP sensor.

interferents, TP and GA were tested due to their electrochemical activity and structural similarity. AA and UA were measured because they largely present in human biological fluids, while XA has an overlapping oxidation potential on the sensor with melatonin. SWV response of solutions having a mixture of melatonin and 5-100 fold interfering substances was recorded at pH 7.2 using imprinted sensor. The oxidation potential for AA, UA, XA, TP and GA were observed at 40 mV, 340 mV, 650 mV, 720 mV and 900 mV, respectively. The experimental results in Fig. 9A showed that no significant changes in the peak current response of melatonin were observed in the presence of these interfering

substances. Fig. 9B shows the SWVs current response of melatonin and other interferents at GCE/GR/MIP and GCE/GR/NIP sensor. The results are indicating that the amount of melatonin bind on GR/MIP sensor is much more than those of comparative interferents. There is only a slight difference between GR/MIP and GR/NIP current response of different interferents. This can be interpreted as the specific integration of melatonin into the complementary imprinting cavities in the imprinted composite. However, other interferents are also showing a slight current response which is possibly attributed to the non-specific adsorption at the GCE/GR/MIP sensor. The relatively higher current response for TP than other interferents is attributed to its similar structure, which makes it to diffuse into the imprinting cavities and cause some non-selective adsorption. The variation of the oxidation peak current of melatonin in all the cases was in the range ± 4%. Thus, it is concluded that, the recognition binding sites formed by the molecular imprinting of guest molecules had the selectivity towards melatonin and selectivity is not due to the difference in redox potential of melatonin and interfering compounds.

Reproducibility and stability of the sensor

To evaluate the reproducibility of the developed sensor, a series of six sensors were prepared for the detection of 10 μM melatonin. The peak current response of melatonin was determined with six sensors under the same conditions (incubating time 4 min). The relative standard deviation (RSD) of the measurements for the six sensors was ± 1.3 %. Good reproducibility of each sensor was indicated after elution and rebinding of the template. Interday precision was also examined by measuring the response of the peak current at the imprinted sensor for 10 consecutive days for the 10 μM concentration of melatonin and the R.S.D. value was found to be ± 2.56%, which confirmed the excellent reproducibility of imprinted sensor.

The stability of the three imprinted sensors was also determined by measuring the voltammetric current response of constant concentration of 10 μM of melatonin, after dipping them over a period of 3 days and 6 days in double distilled water. The current response decreased by 2.23% and 4.31% of its initial value after 3 days and 6 days, respectively. Simultaneously, three imprinted sensors were used to detect 10 μM melatonin solutions every three days for one month. After two weeks, the current response was retained to 95% of the initial value, whereas decreased to 70% after a month. These results suggested that the proposed sensor possessed acceptable storage stability for two weeks.

Analytical applicability of imprinted sensor

Pharmaceutical samples

To demonstrate the analytical applicability of the imprinted sensor in formulations, two commercially available tablet Zytonin 3 mg tablet (Cadila Healthcare Ltd., Ahmedabad, Gujarat) and Eternex 3 mg tablet (Dabur Pharmaceuticals Ltd., Baddi, Himachal Pradesh) were analyzed. The solution of the

Table 2. Determination of melatonin in pharmaceutical samples using imprinted sensor.

Sample	Stated Cotent (mg)	Determined Content (mg)	Error (%)
Eternex	3	2.98	0.6
Zytonin	3	2.97	1.0

tablet samples was prepared by the dissolution in minimum amount of ethanol, followed by sonication for 20 min and then dilution was made with water to obtain final volume. The samples were subsequently diluted with buffer (pH 7.2) so that the concentration of melatonin reached in the working range. Square wave voltammograms were then recorded by incubating

RSC Advances Accepted Manuscript

This journal is © The Royal Society of Chemistry 2012

the imprinted sensor for 4 min in samples under optimized conditions. Keeping dilution factor in consideration, it was found that the observed value of melatonin concentration in pharmaceutical samples was in good agreement with the label contents as shown in Table 2.

Real samples

Melatonin levels are highest during adolescence and begin to decrease in the middle and latter years of life. Melatonin hormone produces by the pineal gland under the influence of the dark/light cycle, is involved in the control of the circadian system. The lower secretion of melatonin in the human body leads to sleeping disorders (insomnia) and Alzheimer's disease. In the earlier studies, it has been suggested that the exogenous melatonin may be a potential treatment for insomnia [46, 47]. However, oral melatonin administration is disadvantageous because of its poor bioavailability, which may result in plasma melatonin concentrations varying up to 25-fold among subjects after application of the same dose. It has been also reported that after oral administration of melatonin, its peak plasma concentration is reached within 1.5 h. The concentration of melatonin in plasma and urine samples of the healthy volunteers, after oral administration of 3-100 mg melatonin tablets has been detected by using RIA techniques and the concentration is found to vary in the range of nM concentration (varied according to oral dose as well as individual volunteers) [12, 48-50]. To examine the practical applicability of the proposed method, the evaluation of melatonin level in the blood plasma of the insomnia patents undergoing treatment with

Table 3. Recovery data for melatonin determination in patient plasma sample at imprinted sensor.

Sr. no.	Spiked (μM)	Observed[a] (μM)	Actual[b] (μM)	Recovery (%)
1.	0	0.078	0.078	----
2.	0.5	0.572	0.072	98.80
3.	1.0	1.083	0.083	100.50
4.	2.0	2.080	0.085	100.35

The R.S.D. value for the determination was less than 1.74% for n=3.
a The observed values are sum of melatonin present + spiked amount.
b The actual amount is observed –spiked amount

melatonin (10 mg dose) has been done. The SWVs were recorded to determine the concentration of melatonin in the plasma samples after dilution with buffer solution in 1:1 ratio. By using standard addition plot, the melatonin concentration was detected in the plasma and the concentration of melatonin was found to be 78 nM (Fig. 10). The negative intercept on the x-axis corresponds to the amount of the analyte in the test sample. This value is given by a/b, the ratio of the intercept and the slope of the regression line. The recovery of melatonin after spiking was also determined and was found in the range of 98.8–100.5% as summarized in Table 3. The excellent recoveries with the low RSD value indicate the accuracy and reproducibility of the proposed method. As melatonin excreted in urine is relatively low [49], the determination is carried out by recovery experiments. For the recovery measurements, urine samples were spiked with known concentrations of standard

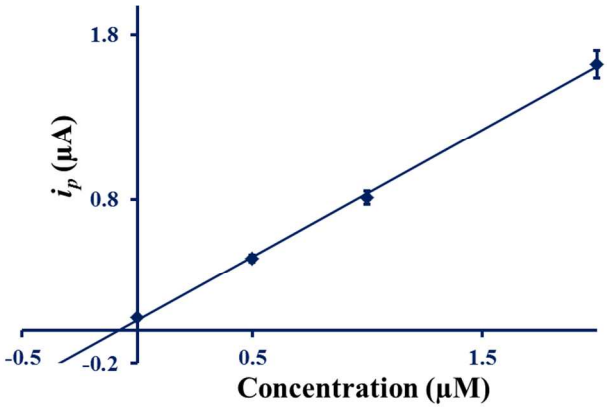

Fig.10 Observed standard addition plot for melatonin concentration in patient plasma sample.

solution of melatonin. Before analysis, the urine samples were diluted 4 times with buffer solution and square wave voltammograms were recorded. The concentration of melatonin in urine samples was then calculated by using regression equation and the results obtained are tabulated in Table 4, showing recovery in the range of 98.5–102.0% with RSD of ± 3.4% (n = 3). Thus, melatonin can be estimated in urine samples using the developed sensors.

Table 4. Recovery data for melatonin determination in urine sample at imprinted sensor.

Sr. no.	Spiked (μM)	Detected (μM)	Recovery (%)
1.	1.0	1.02	102.00
2.	1.5	1.52	101.33
3.	2.0	1.97	98.50

The R.S.D. value for the determination was less than 2.18% for n=3.

Conclusion

A rapid, sensitive and extremely selective electrochemical sensor has been developed for the determination of melatonin by using novel graphene and co-polymer composite as the functional matrix. The prepared sensor displayed a good recognition capacity for template molecule in the presence of other biomolecules. The developed sensor was successfully applied for the determination of melatonin in pharmaceutical formulations and in human biological fluids. The strategy proposed in this work is applicable to determine the nano-molar concentration of melatonin in blood as well as in urine sample. A linear relationship between the melatonin concentration and the current response was obtained at imprinted sensor with excellent reproducibility and a low detection limit of 60×10^{-10} M. In addition, the sensor is selective as no interference from uric acid and ascorbic acid, commonly present in biological

RSC Advances Accepted Manuscript

fluids, is observed. The fabrication procedure of the imprinted sensor is rapid, convenient and eco-friendly, which is essential to the flexible applications. Thus, it is concluded that the proposed molecularly imprinted method can be used as a recognition tool for the selective determination of melatonin with adequate accuracy in clinical and pharmaceutical samples.

Acknowledgment

One of the authors (PG) is thankful to the Ministry of Human Resource Development, New Delhi, for the award of Senior Research Fellowship. The financial assistance for this work was provided by the Department of Biotechnology, Ministry of Science and Technology, NewDelhi vide Grant no. BT/PR13954/MED/32/143/2010.

Notes and references

[a] Department of Chemistry, Indian Institute of Technology Roorkee, Roorkee -247667 (India)
E.Mail : rngcyfcy@iitr.ac.in, Tel: +91-1332-285794 (O) Fax: +91-1332-273560

1 F. A. M. Al-Omary, *Profiles. Drug. Subst. Excip. Relat. Methodol.*, 2013, **38**, 159-226.
2 D. X. Tan, L. C. Manchester, M. P. Terron, L. J. Flores and R. J. Reiter, *J. Pineal Res.*, 2007, **42**, 28-42.
3 A. Radi and G. E. Bekhiet, *Bioeletrochem. Bioenerg.*, 1998, **45**, 275-279.
4 A. Babaei, A. R. Taheri and I. K. Farahani, *Sensors Actuat. B*, 2013, **183**, 265-272.
5 J. R. Johns and J. A. Platts, *Org. Biomol. Chem.*, 2014, **12**, 7820-7827.
6 M. N. Alarcón, F. J. R. Ojeda, R. M. B. Herrera, M. M. A. Serrano, D. A. Castroviejo, G. F. Vázquez, and A. Agil, *Food Funct.*, 2014, **5**, 2806-2832.
7 H. M. Zhang and Y. Zhang, *J. Pineal Res.*, 2014, **57**, 131–146.
8 R. J. Reiter, D. X. Tan, J. C. Mayo, R. M. Sainz, J. Leon and Z. Czarnocki, *Acta Biochim. Pol.*, 2003, **50**, 1129-1146.
9 J. C. Mayo, R. M. Sainz, D. X. Tan, I. Antolín, C. Rodríguez and R. J. Reiter, *Endocrine*, 2005, **27**, 169-178.
10 J. Wang and Z. Wang, *Acta Pharmacol. Sin.*, 2007, **27**, 41–49.
11 A. Levent, *Diamond Relat. Mater.*, 2012, **21**, 114–119.
12 F. Waldhauser, M. Waldhauser, H. R. Lieberman, M. H. Deng, H. J. Lynch and R. J. Wurtman, *Neuroendocrinology*, 1984, **39**, 307-313.
13 E. Chanut, J. N. Legros, C. V. Botteri, J. H. Trouvin and J. M. Launay, *J. Chromatogr. B*, 1998, **709**, 11–18.
14 A. A. Vitale, C. C. Ferrari, H. Aldana and J. M. Affanni, *J. Chromatogr. B*, 1996, **681**, 381-384.
15 G. Simonin, L. Bru, E. Lelievre, J. P. Jeanniot, N. Bromet, B. Walther and C. B. Neyret, *J. Pharm. Biomed. Anal.*, 1999, **21**, 591–601.
16 V. Pucci, A. Ferranti, R. Mandrioli and M. A. Raggi, *Anal. Chim. Acta*, 2003, **488**, 97–105.
17 E. Poboz, A. Michalski, J. S. Brochocka, and M. Trojanowicz, *J. Sep. Sci.*, 2005, **28**, 2165–2172.
18 J. Lu, C. Lau, M. K. Lee and M. Kai, *Anal. Chim. Acta*, 2002, **455**, 193–198.
19 M. Plebani, M. Masiero, A. P. Burlina, M. L. Chiozza, M. Scanarini and A. Burlina, *Child's Nerv. Syst.*, 1990, **6**, 220-221.
20 A. S. Amin, M. Zaky and A. M. E. Beshbeshy, *Mikrochim. Acta*, 2000, **135**, 81-85.
21 B. Agrawal, P. Chandra, R. N. Goyal and Y. B. Shim, *Biosens. Bioelectron.*, 2013, **47**, 307–312.
22 W. X. Ping, Z. Lan, L. W. Rong, D. J. Ping, C. H. Qing and C. G. Nan, *Electroanalysis*, 2002, **14**, 1654-1660.
23 A. L. Saber, *Electroanalysis*, 2010, **22**, 2997-3002.
24 W. Qu, F. Wang, S. Hu and D. Cui, *Microchim. Acta*, 2005, **150**, 109–114.
25 G. O. El-sayed and A. S. Amin, *Lat. Am. J. Pharm.*, 2010, **29**, 1235-1241.
26 J. L. C. Antun, E. M. A. Villar, M. T. F. Abedul, A. C. Garcia, J. *Pharm. Biomed. Anal.*, 2003, **31**, 421-429.
27 D. A. Jimenez, G. D. Diaz, M. C. B. Lopez, M. J. L. Castanon, A. J. M. Ordieres and P. T. Blanco, in: S. Li, Y. Ge, S.A. Piletsky, J. Lunec (Eds.), 2012, 1–34, doi:10.1016/B978-0-444-56331-6.00001-3
28 R. Schirhagl, *Anal. Chem.*, 2014, **86**, 250-261.
29 A. Merkoci and S. Alegret, *Trends Analyt. Chem.*, 2002, **21**, 717-725.
30 S. Piletsky, S. Piletsky and I. Chianella, in: S. Li, Y. Ge, S.A. Piletsky, J. Lunec (Eds.), 2012, 339-354, doi:10.1016/B978-0-444-56331-6.00014-1
31 S. Cao, J. Chen, W. Sheng, W. Wu, Z. Zhao and F. Long, in: S. Li, Y. Ge, S.A. Piletsky, J. Lunec (Eds.), 2012, 57-72, doi:10.1016/B978-0-444-56331-6.00003-7
32 B. J. Sanghavi, W. Varhue, J. L. Chávez, C. F. Chou and N. S. Swami, *Anal. Chem.*, 2014, **86**, 4120-4125.
33 Sanghavi, B. J.; Sitaula, S.; Griep, M. H.; Karna, S. P.; Ali, M. F.; Swami, N. S. *Anal. Chem.* 2013, **85**, 8158-8165.
34 J. Zhu, M. Chen, Q. He, L. Shao, S. Wei and Z. Guo, *RSC Adv.* 2013, **3**, 22790–22824.
35 H. Gao and H. Duan, *Biosens. Bioelectron.*, 2015, **65**, 404–419.
36 J. Luo, S. Jiang and X. Liu, *Sensors Actuat. B*, 2014, **203**, 782–789.
37 Y. Mao, Y. Bao, S. Gan, F. Li and L. Niu, *Biosens. Bioelectron.*, 2011, **28**, 291– 297.
38 H. D. Silva, J. G. Pacheco, J. M. Magalhães, S. Viswanathan, C. D. Matos, *Biosens. Bioelectron.*, 2014, **52**, 56–61.
39 Rosy, H. Chasta, and R. N. Goyal, *Talanta*, 2014, **125**, 167–173.
40 G. D. Christian and W. C. Purdy, *J. Electroanal. Chem.*, 1962, **3**, 363-397.
41 D. C. Marcano, D. V. Kosynkin, J. M. Berlin, A. Sinitskii, Z. Sun, A. Slesarev, L. B. Alemany, W. Lu, and J. M. Tour, *Nano*, 2010, **4**, 4806-4814.
42 Rosy, S. K. Yadav, B. Agrawal, M. Oyama, and R. N. Goyal, *Electrochim. Acta*, 2014, **125**, 622–629.
43 M. Amare and S. Admassie, *Talanta*, 2012, **93**, 122– 128.
44 P. Gupta, R. N. Goyal, *Talanta*, 2014, **120**, 17–22.
45 B. Tang, H. Guoxin and H. Gao, *Appl. Spectrosc. Rev.*, 2010, **45**, 369–407.
46 D. P. Cardinali, A. M. Furio and L. I. Brusco, *Curr. Neuropharmacol.*, 2010, **8**, 218-227.
47 N. L. Rogers, D. F. Dinges, D. J. Kennaway and D. Dawson, *Sleep*, 2003, **26**, 1058-1059.
48 J. G. MacFarlane, J. M. Cleghorn, G. M. Brown and D. L. Streiner, *Biol. Psychiatry*, 1991, **30**, 371-376.
49 O. Vakkuri, J. Leppaluoto and A. Kauppila, *Life Sci.*, 1985, **37**, 489-495.
50 J. Kovacs, W. Brodner, V. Kirchlechner, T. Arif, and F. Waldhauser, *J. Clin. Endocrinol. Metab.*, 1999, **85**, 666-670

RSC Advances Accepted Manuscript

 This journal is © The Royal Society of Chemistry 2012